Macromolecules

ARTICLE

pubs.acs.org/Macromolecules

Ultrahigh Density Array of Free-Standing Poly(3-hexylthiophene) Nanotubes on Conducting Substrates via Solution Wetting

Jinseok Byun, Youngsuk Kim, Gumhye Jeon, and Jin Kon Kim*

National Creative Research Initiative Center for Block Copolymer Self-Assembly, Department of Chemical Engineering, Pohang University of Science and Technology, Pohang, Kyungbuk 790-784, Republic of Korea

Supporting Information

ABSTRACT: An ultrahigh density array of vertically and laterally aligned poly(3-hexylthiophene) (P3HT) nanotubes on conducting substrates was successfully fabricated by solution wetting in the anodized aluminum oxide (AAO) template. After solvent annealing, the conductivity of P3HT nanotubes was significantly increased due to highly aligned P3HT chains along the nanotube direction (or perpendicular to the substrate). This approach also provides a facile route for the preparation of ultrahigh density array of various conjugated polymer nanotubes. The conducting polymer nanotube array could be used for high performance organic devices, such as sensors, organic photovoltaic cells, and electrochromic devices.

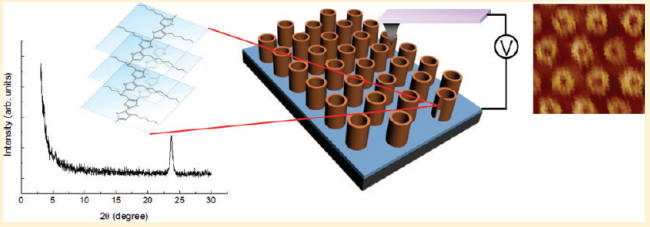

1. INTRODUCTION

Inorganic nanotubes and their arrays have been widely investigated for potential applications to electronics, optoelectronics, nanofluidics, and sensors due to their unique properties and large surface area.[1−8] To fabricate the nanotube array, a variety of synthetic methods such as hydro/solvothermal, sol−gel methods, chemical vapor deposition (CVD), electrochemical anodization, and template-based method have been introduced.[5−10]

Conjugated polymers, for instance poly(3-alkylthiophene), have been widely used for flexible organic devices due to low cost and easy fabrication at low temperatures.[11−14] Their (opto)-electronic, electrochromic, and sensing properties can be greatly enhanced when they are confined to the nanoscale dimensions.[15−19] Especially, vertically and laterally aligned free-standing nanotube array on a conducting substrate would be ideal structures for an active layer of high performance organic photovoltaic cells or sensors and electrodes of electrochromic devices. This is because nanotube array has larger surface area compared to nanorod array. For example, nanotube arrays can be the best geometry for electrochromic devices. These arrays provide short (10−20 nm) diffusion distances for the fast interconversion rate between doped and undoped (or redox) states, while maintaining large surface area.[19] However, compared with inorganic nanotube arrays on conducting substrates, researches on conjugated polymer nanotube array on conducting substrates have been limited because the fabrication of this array is very difficult. Some research groups prepared polymer nanotubes (or nanowires) by using polymer wetting or nanoimprint[20−25] and electropolymerization[19,26−28] to provide nanoscale confinement of polymer chains. Because polymers in melt or solution state could be spontaneously wetted on the wall of nanopores having a high surface energy (for example, anodized aluminum oxide (AAO)),[20−25,29] conducting polymer nanotubes (or nanowires) could be fabricated depending on the molecular weight of the polymer or annealing temperatures. However, in this situation, it is practically impossible to obtain polymer nanotubes with uniform height and controllable wall thickness in a large area (>cm^2). Furthermore, because a thin continuous film layer still remains on the substrate, the nanotubes cannot directly touch the substrate.[30,31]

On the other hand, when the electropolymerization is employed in a nanoporous template such as AAO[32−37] with thin electrodes, nanotubes could directly touch the electrode.[36,37] But, vertically aligned nanotubes inside the template collapse and lose their vertical orientation because the thin electrode cannot act as a rigid support after removal of the AAO template.[36,37] Kim and co-workers[26] fabricated ultrahigh density array of conducting polymer nanorods via electropolymerization inside a nanoporous block copolymer template. However, ultrahigh density array of conducting polymer nanotubes could not be prepared in this system. Moreover, when conjugated polymers, for instance, poly(3-hexylthiophene) (P3HT)), are prepared by the electropolymerization, the regioregularity of the conjugated polymers is significantly decreased.[38] In this situation, the excellent charge transport which is essential for organic (or polymeric) solar cells or sensors cannot be expected for this nanotube array. Thus, a facile and effective route for arrays of free-standing conjugated polymer nanotubes on the conducting substrate, while maintaining excellent charge transfer, has been most needed.

Received: September 5, 2011
Revised: September 28, 2011
Published: October 13, 2011

In this paper, we fabricated a vertically and laterally ordered ultrahigh density array of P3HT nanotubes by solution wetting in the AAO template. It is known that P3HT has been extensively used for high performance organic devices.[39,40] Then, solvent-vapor-assisted P3HT chain alignment was performed, resulting in the enhanced conductivity. Any further thermal treatment, which has been widely used for the enhanced chain orientation of conjugated polymers,[39,40] was not required, and the fabrication process was performed at room temperature. We found that the conductivity of fabricated P3HT nanotubes was ~10 times higher than that of a continuous P3HT film due to the excellent alignment of P3HT chains along the nanotube axis. This method might also be applied to prepare ultrahigh density array of nanotubes of various conjugated polymers. This conjugated polymer nanotube array could be used for highly efficient organic (or polymeric) solar cells, sensors, and electrochromic devices.

2. EXPERIMENTAL SECTION

Fabrication of the P3HT Nanotube Array. An AAO template was prepared by two-step anodization and carefully placed on a surface-modified ITO-coated glass.[33] Dihydroxyl-terminated polystyrene (the weight-average molecular weight (M_w) of 6500 g/mol, Polymer Source, Inc.) was used as a grafting layer to enhance the adhesion between the AAO template and ITO-coated glass.[33] To make the height and diameter of nanopores having 200 and 65 nm, the second anodization time and pore widening time were 2 and 37 min, respectively. It is noted that the AAO templates with various diameters (20−400 nm) of nanopores were easily fabricated by using different eletrolytes.[33,34] A regioregular P3HT (M_w = 29 000 g/mol, Rieke Metals) solution in chloroform ($CHCl_3$) (0.5 wt % in solid) was dropped on the AAO template. After waiting 1 min, the sample was rotated at a speed of 3500 rpm under chloroform vapor environment at room temperature. After rotating, the sample was exposed additionally to the chloroform vapor for 90 min. The AAO template was removed by immersing the sample in aqueous phosphoric acid (H_3PO_4, 5 wt %) solution for 1 h, followed by rinsing with DI water several times. The remaining water was completely removed by freeze-drying to maintain the vertically aligned and free-standing P3HT nanotube array on the ITO-coated glass.

Characterization of the Morphology. The sample was coated with osmium (Osmium coater, Neoc-ST) and examined by using field emission scanning electron microscopy (FE-SEM, Hitachi S-4800) operated at 3 kV. We also employed a transmission electron microscope (TEM, Hitachi-7600) operated at 120 kV and high-resolution TEM (HR-TEM, JEOL JEM-2100F). The out-of-plane GI-XD measurement was performed at Pohang Accelerator Laboratory (PAL) 10C1 beamline with a wavelength of 1.54 Å. The exposure time was 2 s with an increment of $2\theta = 0.02°$ in the range of 2θ between 3° and 25°. The χ scan was performed at fixed $2\theta = 23.3°$ with intervals from 45° to 135°. The exposure time was 10 s with the increment of 0.1°.

Measurement of the Current of Each Nanotube. The current of the individual nanotube was measured by current-sensing atomic force microscopy (CS-AFM; Aglient Technologies, Inc.) at an applied direct current bias of 1 V with a conductive Pt-coated ultrasharp silicon AFM tip on cantilevers. For these measurements, only the top part of (25 nm) the AAO template was removed by using 9 wt % of aqueous H_3PO_4 for 5 min at 35 °C.

3. RESULTS AND DISCUSSION

Figure 1 shows a schematic for the preparation of the ultrahigh density array of P3HT nanotubes via solution wetting. First, the AAO template with highly ordered pores (diameter and height of pores are 65 and 200 nm, respectively) in the large area (>cm^2)

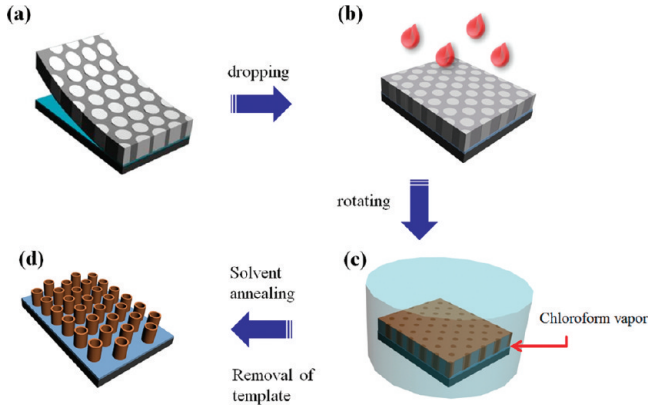

Figure 1. Schematic for the fabrication of the P3HT nanotube array.

was prepared on the ITO-coated glass (Figure 1a).[33] Then, P3HT solution in chloroform was dropped onto the AAO template to infiltrate nanopores. Since the wall of the AAO template has high surface energy, the polymer solution could be wetted spontaneously.[20,29] After all the nanopores were completely infiltrated by P3HT solution, the excess polymer solution located at the top part of the template was removed by rotating the sample (Figure 1b). However, a thin wetting layer existed on the top part of the AAO template even after the rotation. Next, the sample was exposed to chloroform vapor for 90 min (Figure 1c). During this process, P3HT chains located near the top part of the AAO template could infiltrate the template due to the lower viscosity of P3HT under the solvent vapor. A similar approach has been used for room temperature and low-pressure imprinting process.[41] Another purpose of the use of solvent annealing is to suppress a fast solvent evaporation;[42,43] thus, fabricated P3HT nanotubes maintained high crystallinity. Finally, the AAO template was removed by wet-etching, and residual water was completely removed by the freeze-drying method,[33] generating a laterally and vertically aligned ultrahigh density array of free-standing P3HT nanotubes on the ITO-coated glass (Figure 1d).

Figures 2a and 2b show top and cross-sectional field emission scanning electron microscope (FE-SEM) images of the ultrahigh density array of free-standing P3HT nanotubes on the ITO-coated glass. The diameter and height of each P3HT nanotube are 65 and 200 nm, respectively, which are exactly the same as those of the AAO template. Since the AAO templates with wide ranges of the pore size (20−400 nm in the diameter) and the height (200 nm~1 μm) were easily fabricated,[33,34] the diameter and height of P3HT nanotubes could be easily controlled. The wall thickness of each P3HT nanotube is 16 nm (Figure 2a), and it could be further tuned by changing concentration of P3HT solution (see section 1 of the Supporting Information). The height and wall thickness of P3HT nanotubes measured by the transmission electron microscope (TEM) image (Figure 2c) are consistent with those measured by FE-SEM.

Several research groups have shown that electrical properties of conjugated polymers are greatly enhanced when polymer chains are confined in cylindrical nanorods (or nanowires).[17−19,26,30] To measure the conductivity of the individual nanotube, we used CS-AFM. Because a lateral force was applied to P3HT nanotubes during the measurement, the vertically aligned P3HT nanotube array could be significantly distorted, making the current mapping less accurate. We overcame this difficulty by removing only the top part (25 nm from total 200 nm height) of the AAO template by

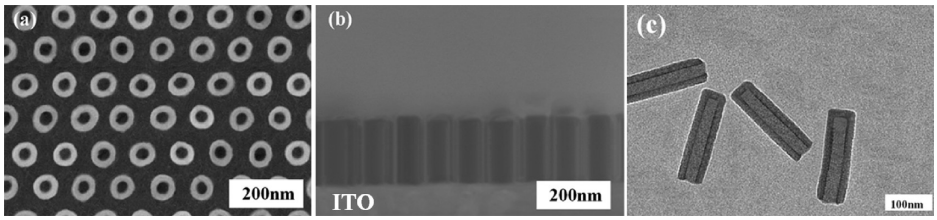

Figure 2. Top (a) and cross-sectional (b) SEM images of P3HT nanotube array onto the ITO glass. (c) TEM image of individual P3HT nanotube.

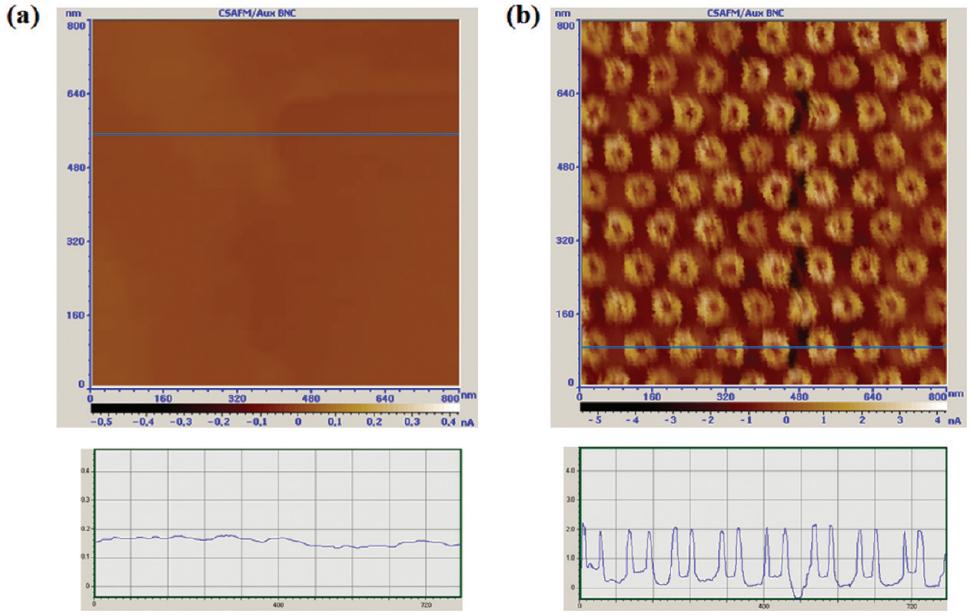

Figure 3. Current-sensing AFM images (top) and profiles (bottom) of the P3HT (a) continuous film and (b) nanotube array.

careful control of wet-etching time.[44] We found that P3HT nanotubes were maintained against the lateral force during the current mapping. Figures 3a and 3b are current images and profiles of the continuous P3HT film and ultrahigh density array of P3HT nanotubes at an applied direct current bias of 1 V. The continuous film sample was also prepared by spin-coating followed by chloroform vapor annealing for 90 min (see section 2 in the Supporting Information). The current image of P3HT nanotubes shows that the current flows only through the wall of nanotubes. The current through each P3HT nanotube was ~2 nA, which is 10 times higher than that (~0.18 nA) of the continuous P3HT film. Interestingly, the P3HT nanotube array showed very uniform current flow, indicating that P3HT nanotubes have uniform height through the entire area.

We also measured the conductivity of P3HT nanotubes with the two-point probe method (see Supporting Information, section 3). Conductivity is given by the conductance, which is the slope of the current versus voltage ($I-V$) curve, divided by the contact area. To compare the conductivity of the P3HT nanotube array with that of the continuous P3HT film, the same constant electrode area (6.18×10^{-4} cm^2) and height (200 nm) should be used. We found that the conductance of P3HT nanotubes is 2.8 times higher than that of the continuous film (Figure 4). Since the contact area of P3HT nanotubes to the electrode is only 28.5% that of the continuous P3HT film (see Supporting Information, section 3), the conductivity (3.88×10^{-3} S/cm) of P3HT nanotubes is 10 times higher than that

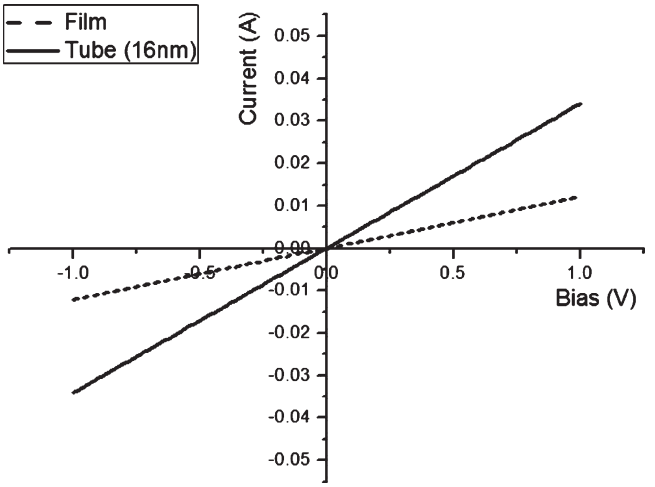

Figure 4. $I-V$ curves for the P3HT continuous film and P3HT nanotube array measured by two-point probe experiment.

(3.94×10^{-4} S/cm) of the continuous film, which is consistent with the result observed in the CS-AFM measurement.

Since the great enhancement of the conductivity is related to the chain orientation inside the polymer nanotube, we performed grazing incidence X-ray diffraction (GI-XD) and high-resolution transmission electron microscope (HR-TEM) experiments. The P3HT continuous film showed a distinct peak (Supporting

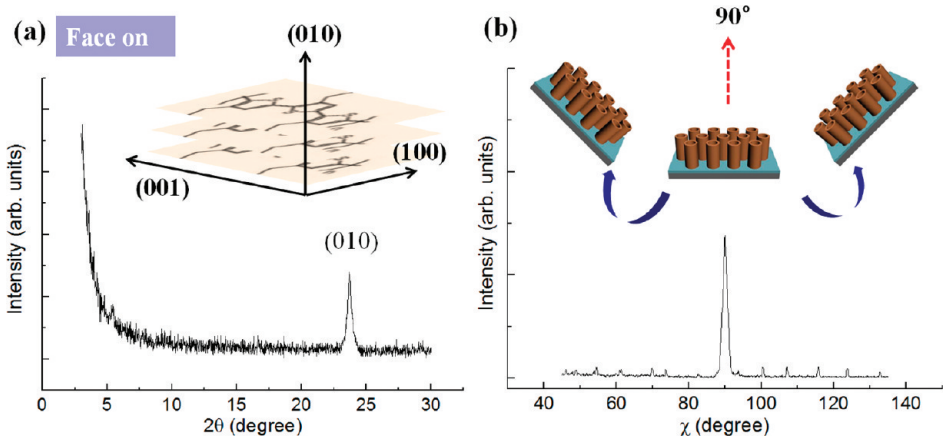

Figure 5. (a) Out-of-plane grazing incidence angle X-ray diffraction patterns as a function of the scattering angle 2θ for the P3HT nanotube array. (b) χ dependence of X-ray diffraction of the P3HT nanotube array.

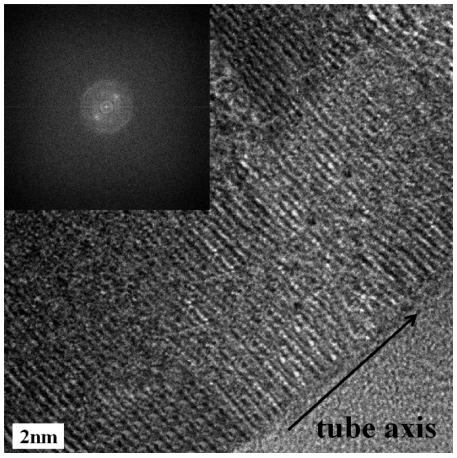

Figure 6. HR-TEM image of the single P3HT nanotube and SAED pattern (inset).

Information, section 2) at $2\theta = 5.4°$, which is the lamellar layer structure ((100) plane) with a spacing of 16.8 Å. The continuous film was also prepared by chloroform vapor for 90 min, which is the same condition employed for the fabrication of the nanotube. This XRD pattern indicates that P3HT lamellae stand on the substrate (edge-on conformation), consistent with previous results.[39,40,42,43] But, the XRD pattern of the P3HT nanotube array (Figure 5a) shows a distinct peak at $2\theta = 23.3°$ (the lattice spacing of 3.8 Å), corresponding to the (010) plane of P3HT, arising from the $\pi-\pi$ interchain stacking.[39,40,42,43] This indicates that the $\pi-\pi$ stacking is highly aligned perpendicular to the substrate (face-on conformation of the P3HT lamellae on the substrate). We performed χ scan at fixed 2θ (23.3°) to further investigate the distribution of the face-on conformation with respect to the substrate. The distribution of the $\pi-\pi$ stacking in P3HT nanotubes shows a very sharp peak at $\chi = 90°$ (Figure 5b). This indicates that highly oriented face-on conformation to the substrate was formed, where the $\pi-\pi$ stacking is aligned along the nanotube axis.

Figure 6 gives HR-TEM image of single P3HT nanotube and the selected area electron diffraction (SAED) pattern. The distance between two adjacent lines in the HR-TEM image is ~3.8 Å, which is identical to the $\pi-\pi$ stacking distance.[39,40] Furthermore, the existence of only two spots in the SAED pattern indicates that the $\pi-\pi$ stacking is highly oriented along the tube axis (or perpendicular to the substrate), which is consistent with results given in Figure 5.

We considered that highly aligned P3HT chains along the nanotube direction might be achieved by the surface interaction between P3HT chains and the wall of the AAO template. It is well-known that the edge-on conformation of P3HT lamellae is an equilibrium state in the continuous thin film on the substrate, which provides an excellent electrical charge transport parallel to the substrate.[39,40,42,43] This is because the repulsion force is anticipated at the interface between hydrophobic hexyl side chains in the P3HT and a hydrophilic substrate (for instance, AAO wall or silicon oxide).[39] Thus, during the solvent evaporation the conformation of the hexyl side chains in the P3HT should be adjusted to minimize the contact to the hydrophilic substrate. This leads to the edge-on conformation of the P3HT chains to the hydrophilic substrate.[39] If this concept is applied to cylindrical confinement, the AAO wall could act as the surface of the continuous film. Then, P3HT lamellae near the wall prefer to have the edge-on structure perpendicular to the tube axis, namely, the face-on conformation along the nanotube axis. We found that the alignment of the $\pi-\pi$ stacking along the nanotube axis was greatly enhanced with increasing solvent annealing times (see section 4 in the Supporting Information). At short annealing times, P3HT chains in the nanotube have mixed orientations of edge-on and face-on conformations because of an insufficient time to achieve the equilibrium state. However, with increasing annealing time, almost all of P3HT chains in nanotubes exhibited the face-on conformation along the tube axis. Because the P3HT chains should be confined in the nanopores, the perpendicular $\pi-\pi$ stacking is easy to be obtained with the high crystallinity. Therefore, a significant increase of the current flow, as shown in Figure 3, is attributed to the fact that most of the P3HT nanotubes have the $\pi-\pi$ stacking perpendicular to the substrate.

4. CONCLUSION

In summary, we fabricated a highly ordered free-standing P3HT nanotube array on the conducting substrate by solution wetting inside the AAO template. Because the AAO template used in this study has very uniform pore size and height, highly ordered P3HT nanotube array could be fabricated in the large

area. P3HT lamellae in the nanotubes have the face-on chain conformation to the substrate (the $\pi-\pi$ stacking is along the tube axis) due to the interaction between P3HT chains and the wall. Because the $\pi-\pi$ stacking in nanotubes is highly aligned along the nanotube axis, the conductivity was greatly enhanced (~10 times) compared with that of the continuous film. This method could be also applied to prepare the ultrahigh density array of nanotubes of various conjugated polymers. This array could be used as highly efficient organic (or polymeric) solar cells, sensors, and electrochromic devices.

■ ASSOCIATED CONTENT

Supporting Information. Details on the two-point probe experiment, calculation of the contact area of P3HT nanotube to the electrode, effect of the solvent annealing time on the chain orientation. This material is available free of charge via the Internet at http://pubs.acs.org.

■ AUTHOR INFORMATION

Corresponding Author
*E-mail: jkkim@postech.ac.kr.

■ ACKNOWLEDGMENT

This work was supported by the National Creative Research Initiative Program of the National Research Foundation of Korea (NRF). GI-XD experiment was performed at PLS beamline 10C1 supported by NRF and POSCO.

■ REFERENCES

(1) Tremel, W. *Angew. Chem., Int. Ed.* **1999**, *38*, 2175.
(2) Wang, J.; Lin, Z. *Chem. Mater.* **2010**, *22*, 579.
(3) Mor, G. K.; Varghese, O. K.; Paulose, M.; Shankar, K.; Grimes, C. A. *Sol. Energy Mater. Sol. Cells.* **2006**, *90*, 2011.
(4) Rao, C. N. R.; Govindaraj, A. *Adv. Mater.* **2009**, *21*, 4208.
(5) Varghese, O. K.; Paulose, M.; Grimes, C. A. *Nature Nanotechnol.* **2009**, *4*, 592.
(6) Mohapatra, S. K.; John, S. E.; Banerjee, S.; Misra, M. *Chem. Mater.* **2009**, *21*, 3048.
(7) Yu, J.; Wang, F.; Wang, Y.; Gao, H.; Li, J.; Wu, K. *Chem. Soc. Rev.* **2010**, *39*, 1513.
(8) Tan, L. K.; Kumar, M. K.; An, W. W.; Gao, H. *ACS Appl. Mater. Interfaces* **2010**, *2*, 498.
(9) Lei, Y.; Yeong, K.-S.; Thong, J. T. L.; Chim, W.-K. *Chem. Mater.* **2004**, *16*, 2757.
(10) Tan, L. K.; Chong, M. A. S.; Gao, H. *J. Phys. Chem. C* **2008**, *112*, 69.
(11) Sirringhaus, H.; Brown, P. J.; Friend, R. H.; Nielsen, M. M.; Bechgaard, K.; Langeveld-Voss, B. M. W.; Spiering, A. J. H.; Janssen, R. A. J.; Meijer, E. W.; Herwig, P.; de Leeuw, D. M. *Nature* **1999**, *401*, 685.
(12) Yang, X.; Loos, J. *Macromolecules* **2007**, *40*, 1353.
(13) Woo, C. H.; Thompson, B. C.; Kim, B. J.; Toney, M. F.; Fréchet, J. M. J. *J. Am. Chem. Soc.* **2008**, *130*, 16324.
(14) Thompson, B. C.; Kim, B. J.; Kavulak, D. F.; Sivula, K.; Mauldin, C.; Fréchet, J. M. J. *Macromolecules* **2007**, *40*, 7425.
(15) Forzani, E. S.; Zhang, H.; Nagahara, L. A.; Amlani, I.; Tsui, R.; Tao, N. *Nano Lett.* **2004**, *4*, 1785.
(16) Cannon, J. P.; Bearden, S. D.; Gold, S. A. *Synth. Met.* **2010**, *160*, 2623.
(17) Kim, K.; Shin, J. W.; Lee, Y. B.; Cho, M. Y.; Lee, S. H.; Park, D. H.; Jang, D. K.; Lee, C. J.; Joo, J. *ACS Nano* **2010**, *4*, 4197.
(18) Samitsu, S.; Shimomura, T.; Heike, S.; Hashizume, T.; Ito, K. *Macromolecules* **2010**, *43*, 7891.
(19) Cho, S. I.; Kwon, W. J.; Choi, S.-J.; Kim, P.; Park, S.-A.; Kim, J.; Son, S. J.; Xiao, R.; Kim, S.-H.; Lee, S. B. *Adv. Mater.* **2005**, *17*, 171.
(20) Steinhart, M.; Wehrspohn, R. B.; Gösele, U.; Wendorff, J. H. *Angew. Chem., Int. Ed.* **2004**, *43*, 1334.
(21) Steinhart, M.; Senz, S.; Wehrspohn, R. B.; Gösele, U.; Wendorff, J. H. *Macromolecules* **2003**, *36*, 3646.
(22) Shin, K.; Xiang, H.; Moon, S. I.; Kim, T.; McCarthy, T. J.; Russell, T. P. *Science* **2004**, *306*, 76.
(23) Xiang, H.; Shin, K.; Kim, T.; Moon, S. I.; McCarthy, T. J.; Russell, T. P. *Macromolecules* **2005**, *38*, 1055.
(24) Byun, J.; Kim, N.-H.; Lee, D. H.; Lee, K.-H.; Kim, J. K. *Soft Matter* **2009**, *5*, 3835.
(25) García-Gutiérrez, M.-C.; Linares, A.; Hernández, J. J.; Rueda, D. R.; Ezquerra, T. A.; Poza, P.; Davies, R. J. *Nano Lett.* **2010**, *10*, 1472.
(26) Lee, J. I.; Cho, S. H.; Park, S.-M.; Kim, J. K.; Kim, J. K.; Yu, J.-W.; Kim, Y. C.; Russell, T. P. *Nano Lett.* **2008**, *8*, 2315.
(27) Kim, J. K.; Lee, J. I.; Lee, D. H. *Macromol. Res.* **2008**, *16*, 267.
(28) Kim, J. K.; Yang, S. Y.; Lee, Y.; Kim, Y. *Prog. Polym. Sci.* **2010**, *35*, 1325.
(29) Zhang, M.; Dobriyal, P.; Chen, J.-T.; Russell, T. P.; Olmo, J.; Merry, A. *Nano Lett.* **2006**, *6*, 1075.
(30) Kim, J. S.; Park, Y.; Lee, D. Y.; Lee, J. H.; Park, J. H.; Kim, J. K.; Cho, K. *Adv. Funct. Mater.* **2010**, *20*, 540.
(31) Haberkorn, N.; Weber, S. A. L.; Berger, R.; Theato, P. *ACS Appl. Mater. Interfaces* **2010**, *2*, 1573.
(32) Masuda, H.; Fukuda, K. *Science* **2002**, *268*, 1466.
(33) Byun, J.; Lee, J. I.; Kwon, S.; Jeon, G.; Kim, J. K. *Adv. Mater.* **2010**, *22*, 2028.
(34) Jeon, G.; Yang, S. Y.; Byun, J.; Kim, J. K. *Nano Lett.* **2011**, *11*, 1284.
(35) Lei, Y.; Yang, S.; Wu, M.; Wilde, G. *Chem. Soc. Rev.* **2011**, *40*, 1247.
(36) Xiao, R.; Cho, S. I.; Liu, R.; Lee, S. B. *J. Am. Chem. Soc.* **2007**, *129*, 4483.
(37) Fu, M.; Zhu, Y.; Tan, R.; Shi, G. *Adv. Mater.* **2001**, *13*, 1874.
(38) Ratcliff, E. L.; Jenkins, J. L.; Nebesny, K.; Armstrong, N. R. *Chem. Mater.* **2008**, *20*, 5796.
(39) Kim, D. H.; Park, Y. D.; Jang, Y.; Yang., H.; Kim, Y. H.; Han, J. I.; Moon, D. G.; Park, S.; Chang, T.; Chang, C.; Joo, M.; Ryu, C. Y.; Cho, K. *Adv. Funct. Mater.* **2005**, *15*, 77.
(40) Kim, D. H.; Jang, Y.; Park, Y. D.; Cho, K. *Macromolecules* **2006**, *39*, 5843.
(41) Voicu, N. E.; Ludwigs, S.; Crossland, E. J. W.; Andrew, P.; Steiner, U. *Adv. Mater.* **2007**, *19*, 757.
(42) Yang, H.; Shin, T. J.; Yang, L.; Cho, K.; Ryu, C. Y.; Bao, Z. *Adv. Funct. Mater.* **2005**, *15*, 671.
(43) Yang, H.; LeFevre, S. W.; Ryu, C. Y.; Bao, Z. *Appl. Phys. Lett.* **2007**, *90*, 172116.
(44) Erts, D.; Polyakov, B.; Daly, B.; Morris, M. A.; Ellingboe, S.; Boland, J.; Holmes, J. D. *J. Phys. Chem. B* **2006**, *110*, 820.